ACS APPLIED MATERIALS & INTERFACES

Research Article

www.acsami.org

Efficiency Enhancement of Polymer Solar Cells by Applying Poly(vinylpyrrolidone) as a Cathode Buffer Layer via Spin Coating or Self-Assembly

Haitao Wang, Wenfeng Zhang, Chenhui Xu, Xianghong Bi, Boxue Chen, and Shangfeng Yang*

Hefei National Laboratory for Physical Sciences at Microscale, CAS Key Laboratory of Materials for Energy Conversion & Department of Materials Science and Engineering, University of Science and Technology of China (USTC), Hefei 230026, People's Republic of China

Supporting Information

ABSTRACT: A non-conjugated polymer poly(vinylpyrrolidone) (PVP) was applied as a new cathode buffer layer in P3HT:PCBM bulk heterojunction polymer solar cells (BHJ-PSCs), by means of either spin coating or self-assembly, resulting in significant efficiency enhancement. For the case of incorporation of PVP by spin coating, power conversion efficiency (PCE) of the ITO/PEDOT:PSS/P3HT:PCBM/PVP/Al BHJ-PSC device (3.90%) is enhanced by 29% under the optimum PVP spin-coating speed of 3000 rpm, which leads to the optimum thickness of PVP layer of ~3 nm. Such an efficiency enhancement is found to be primarily due to the increase of the short-circuit current (J_{sc}) (31% enhancement), suggesting that the charge collection increases upon the incorporation of a PVP cathode buffer layer, which originates from the conjunct effects of the formation of a dipole layer between P3HT:PCBM active layer and Al electrodes, the chemical reactions of PVP molecules with Al atoms, and the increase of the roughness of the top Al film. Incorporation of PVP layer by doping PVP directly into the P3HT:PCBM active layer leads to an enhancement of PCE by 13% under the optimum PVP doping ratio of 3%, and this is interpreted by the migration of PVP molecules to the surface of the active layer via self-assembly, resulting in the formation of the PVP cathode buffer layer. While the formation of the PVP cathode buffer layer is fulfilled by both fabrication methods (spin coating and self-assembly), the dependence of the enhancement of the device performance on the thickness of the PVP cathode buffer layer formed by self-assembly or spin coating is different, because of the different aggregation microstructures of the PVP interlayer.

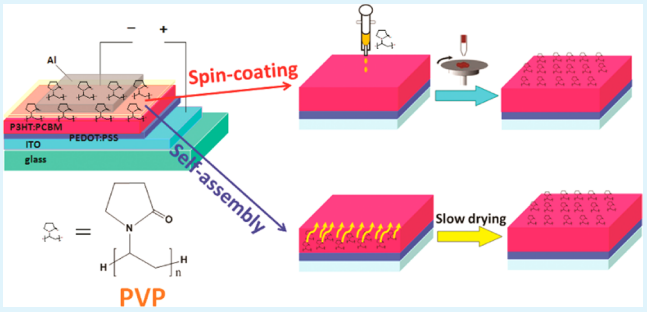

KEYWORDS: *polymer solar cells, poly(vinylpyrrolidone), spin coating, self-assembly, power conversion efficiency, cathode buffer layer*

INTRODUCTION

Polymer solar cells (PSCs) have been receiving great attention in recent years, because it has many advantages compared to the traditional inorganic solar cells, including light weight, flexibility, and low manufacturing cost by the large-area roll-to-roll production process.[1−9] Bulk heterojunction (BHJ) structure comprising an interpenetrating network of a conjugated polymer donor such as poly(3-hexylthiophene-2,5-diyl) (P3HT) and a soluble fullerene acceptor, which is typically [6,6]-phenyl-C61-butyric acid methyl ester (PCBM) as the photoactive layer, has been demonstrated to be the most popular architecture of PSCs reported so far.[1−10] Because of the energy level offsets of donor/acceptor and donor-(acceptor)/electrodes, BHJ-PSCs generally suffer from the pronounced potential loss leading to the limited efficiency. While the design of novel low-band-gap polymers is currently the major approach for the fine tuning of the energy levels of donors, the interfaces between donor(acceptor)/electrodes are determinative for the efficient charge transport and extraction and, hence, are fundamentally important. Ideally, an ohmic contacts at both the anode and cathode electrodes is necessary for efficient charge extraction; otherwise, significant charge accumulation and, consequently, recombination loss of charge carriers would take place.[11−15]

To optimize the interfaces between donor(acceptor)/electrodes, buffer layers or interfacial layers are usually utilized as functional layers between the active layer and electrodes interfaces to facilitate charge collection and extraction by means of inducing interfacial charge redistribution, geometry modifications, and/or chemical reactions have been demonstrated to be essential for achieving maximum performance in PSCs.[11−15] In particular, cathode buffer layers, which are applied between the active layer and cathode, have been extensively investigated to improve the cathode electrode

Received: July 21, 2012
Accepted: December 12, 2012
Published: December 12, 2012

   dx.doi.org/10.1021/am302317v | ACS Appl. Mater. Interfaces 2013, 5, 26−34

efficiency in collecting and extracting negative charge carriers. To date, the materials of cathode buffer layers reported in BHJ-PSCs include alkali-metal compounds such as LiF,[16,17] metal oxides such as TiO_x,[18,19] and organic materials.[20−32] Among them, few studies on using nonconjugated insulating polymers as cathode buffer layers have been reported. In 2007, Zhang et al. reported the first study of inserting a thin cathode buffer layer between the active polymer layer and the metal cathode by spin-coating a nonconjugated polymer, poly(ethylene oxide) (PEO). The open-circuit voltage (V_{oc}) was dramatically enhanced by up to 200 mV, and a noticeable enhancement of the fill factor (FF) and the short-circuit current (J_{sc}) were observed as well, resulting in the enhancement of the power conversion efficiency (PCE) by 50%. They proposed that PEO had a similar function as LiF, i.e., the built-in-potential was increased upon inserting the PEO interfacial layer and thus improving charge transportation.[27] More recently, by incorporating alcohol/water-soluble poly [(9,9-bis(3′-(*N*,*N*-dimethylamino) propyl)-2,7-fluorene)-*alt*-2,7-(9,9-dioctylfluorene)] (PFN) via spin coating as a cathode buffer layer in the BHJ-PSC device based on [6,6]-phenyl C71-butyric acid methyl ester (PC71BM) and thieno[3,4-b]-thiophene/benzodithiophene (PTB7), Wu et al. achieved a certified PCE as high as 8.37%.[28] The reason for the improvement of device performance by the PFN cathode buffer layer was interpreted by the conjunct effects of an enhanced built-in potential across the device because of the existence of interface dipole, improved charge-transport properties, elimination of the buildup of space charge, and reduced recombination loss due to the increase in built-in field and charge carrier mobility.[28] Alternatively, formation of cathode buffer layer in BHJ-PSCs via self-assembly or the so-called spontaneous vertical phase separation was also reported in several studies. Chen et al. found that a thin cathode buffer layer of poly(ethylene glycol) (PEG) was formed by adding up to 5 wt % of PEG to the P3HT:PCBM solution followed by the spontaneous migration of PEG to the surface of the active layer. The PEG cathode buffer layer reduced the contact resistance after undergoing chemical reactions with the Al atoms of the cathode, leading to the improvement of the efficiency of electron collection and, consequently, the enhancement of the PCE.[29] A similar self-organization behavior was also reported in the PSC device containing poly(dimethylsiloxane)-*block*-poly(methyl methacrylate) (PDMS-*b*-PMMA) as a cathode buffer layer, which was initially mixed into the P3HT:PCBM active layer solution and then surface-segregated from the active layer because of the low surface energy of the PDMS block. A plausible interpretation of the enhancement of the PCE was that the PDMS-*b*-PMMA interface layer suppressed charge carrier recombination at the organic/metal interface, but the detailed mechanism is not clear.[30] Besides, fullerene end-capped PEG was also reported by two groups independently to form cathode buffer layer via self-assembly, resulting in not only significant enhancement of the P3HT:PCBM device performance, but also improved thermal stability.[31,32] The enhancement of the device performance upon the addition of fullerene end-capped PEG was mainly attributed to the increase of V_{oc} and FF, which is due to the generation of the interfacial dipole moment and the improved vertical morphology of the P3HT:PCBM active layer with the uniform distribution of PCBM crystallites in the P3HT matrix, respectively.[31,32] Noteworthy, the types of the nonconjugated polymers as the cathode buffer layers reported in the above studies have been quite limited, and the polymer buffer layers are incorporated into the BHJ-PSC devices via either spin coating or self-assembly. Thus, two intriguing questions are raised:

Can other nonconjugated polymers be used as cathode buffer layers?

Is the effect of the polymer cathode buffer layer on the device performance dependent on the fabrication method of spin coating or self-assembly?

In this paper, we report, for the first time, the application of poly(vinylpyrrolidone) (PVP) as a new cathode buffer layer of nonconjugated polymer in P3HT:PCBM BHJ-PSCs, leading to significant efficiency enhancement. PVP was incorporated between the P3HT:PCBM active layer and the Al electrode by means of either spin coating or self-assembly, and the difference on the effect of PVP cathode buffer layer between these two fabrication methods is compared and discussed. The mechanism of the efficiency enhancement upon the incorporation of PVP cathode buffer layer is proposed.

EXPERIMENTAL SECTION

Materials. All materials regarding the device based on the P3HT:PCBM BHJ-solar cells were as follows. The indium tin oxide (ITO) glass substrate with a sheet resistance of 8 Ω/□ was purchased from Shenzhen Nan Bo Group, China. Poly(3,4-ethylenedioxythiophene):polystyrene sulfonic acid (PEDOT:PSS) (Baytron P) was obtained from SCM Industrial Chemical Co., Ltd. Poly(3-hexylthiophene) (P3HT) and (6,6)-phenyl-C61 butyric acid methyl ester ($PC_{61}BM$) was purchased from Luminescence Technology Corp. and Nichem Fine Technology Co., Ltd, respectively. PVP (K30, M_n = ca. 40 000) was purchased from Sinopharm Chemical Reagent Co., Ltd.

Device Fabrication. Our detailed fabrication procedure of the P3HT:PCBM BHJ-PSCs has been reported recently.[33] In brief, the cleaned ITO-coated glass substrate was first treated by ozone−ultraviolet cleaner; then, a thin film (∼45 nm thick) of PEDOT:PSS was spin-coated onto the ITO substrate and then annealed at 120 °C for 30 min. The P3HT:PCBM (1:0.8 w/w) blend was dissolved in chlorobenzene by stirring at 40 °C until all the materials dissolved. The incorporation of PVP layer was carried out using two different methods of spin coating or self-assembly:

(1) The P3HT:PCBM active layer (∼ 90 nm thick) was first fabricated by spin-coating P3HT:PCBM solution in chlorobenzene onto the PEDOT:PSS layer. Then, PVP dissolved in methanol (or isopropyl alcohol) with a concentration of 1 mg/mL was spin-coated onto the P3HT:PCBM active layer at different spin-coating speeds (3000, 3000, and 5000 rpm);

(2) PVP was doped in P3HT:PCBM solution in chlorobenzene with variable weight ratios (1, 3, 5 wt %). To fabricate the PVP-doped active layer via the "slow drying" method, P3HT:PCBM:PVP solution was spin-coated onto the PEDOT:PSS layer at a low spin-coating speed of 800 rpm for 60 s; then, the as-spun wet film was covered with a Petri dish and allowed to stand for 1 h in nitrogen atmosphere.

All of the other solution processing and film preparation was carried out in an air atmosphere. The device was then transferred into a vacuum chamber (∼10^{-5} Torr), and an Al electrode (∼100 nm thick) was deposited on the top of the PVP buffer layer through a shadow mask to define the active area of the devices (2 mm × 5 mm). Finally, thermal annealing was carried out at 150 °C for 10 min inside a vacuum drying oven.

Measurements and Characterization. PCE was measured under simulated AM 1.5 irradiation (100 mW cm^{-2}), using a standard xenon-lamp-based solar simulator (Oriel Sol 3A, USA), for which the illumination intensity was calibrated by a monocrystalline silicon reference cell (Oriel P/N 91150 V, with KG-5 visible color filter) calibrated by the National Renewable Energy Laboratory (NREL).

Scheme 1. Device Architecture of ITO/PEDOT:PSS/P3HT:PCBM/PVP/Al BHJ-PSC Devices with the Incorporation of PVP Buffer Layer via Spin Coating (I) or Self-Assembly (II)

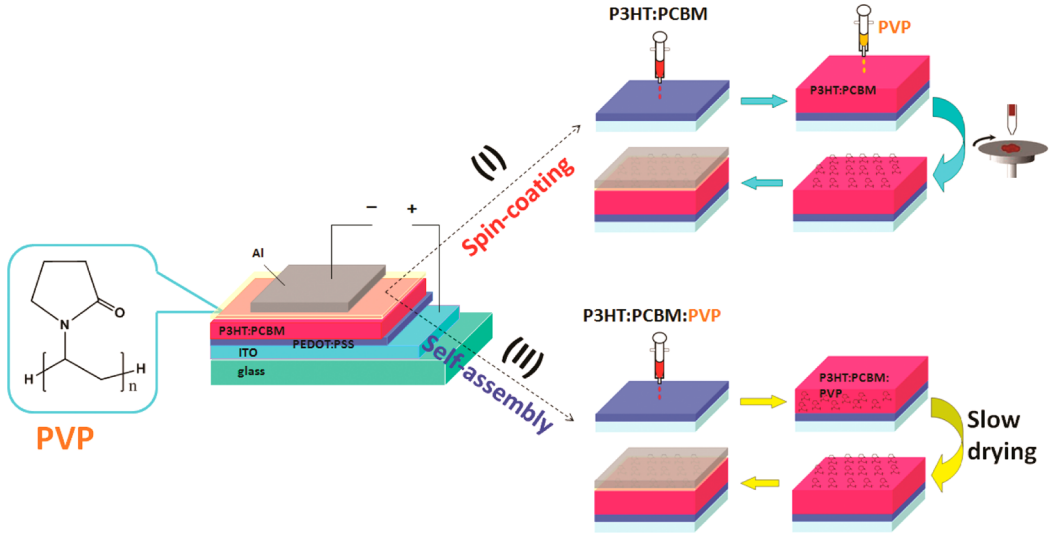

The current–voltage (J–V) characteristics were measured with a Keithley Model 2400 source meter. All the measurements were carried out in an air atmosphere, and a mask with a well-defined area size of 10.0 mm^2 was attached onto the cell to define the effective area, to ensure accurate measurement. More than 10 devices were fabricated independently under each experimental condition and measured to ensure the consistency of the data, and the averaged data were used in the following discussions.

Scanning electron microscope (SEM) images were taken on a Sirion 200 system (FEI, USA) operating at an accelerating voltage of 5 kV. Atomic force microscopy (AFM) measurements were performed using a Digital Instruments system, and AFM images were obtained in contact mode on a Veeco di-Innova scanning probe microscope. The thickness of PVP layers was estimated either by AFM measurement, using a sharp blade to generate ~10 μm wide cuts in the layer, or by a KLA-Tencor P6 surface profilometer. Scanning Kelvin probe microscopy (SKPM) measurements were carried out on AFM equipment, using the standard SKPM mode.

RESULTS AND DISCUSSION

Performances of P3HT:PCBM BHJ-PSCs with PVP Cathode Buffer Layer Incorporated via Spin Coating. In the first series of study, we incorporated a PVP cathode buffer layer between the P3HT:PCBM active layer and Al electrode by means of spin coating (see method (I) in Scheme 1). PVP dissolved in methanol with a concentration of 1 mg/mL was spin-coated onto the P3HT:PCBM active layer at different speeds (1000, 3000, and 5000 rpm), to investigate the effect of the PVP layer and its thickness on device performance. The ITO/PEDOT:PSS/P3HT:PCBM/PVP/Al BHJ-PSC devices thus constructed were annealed and measured in air atmosphere under simulated AM 1.5 irradiation (100 mW cm^{-2}). The current–voltage (J–V) curves of ITO/PEDOT:PSS/P3HT:PCBM/PVP/Al BHJ-PSCs fabricated at different spin-coating speed of PVP are compared in Figure 1, and the measured parameters (J_{sc}, V_{oc}, FF, PCE) based on the average of 6~10 devices fabricated independently under each experimental condition are summarized in Table 1. Compared to the reference ITO/PEDOT:PSS/P3HT:PCBM/Al device (reference) without the incorporation of any cathode buffer layer which exhibits a PCE of 3.03%, clearly our devices incorporated by PVP cathode buffer layer (PVP-1000, PVP-3000, and PVP-5000, which corresponds to the spin-coating speed of 1000, 3000, and 5000 rpm, respectively) all exhibit the enhancement of PCE. With the increase of the spin-coating speed of PVP from 1000 rpm to 3000 rpm, PCE of the PVP-incorporated devices increases dramatically (3.50% and 3.90% for PVP-1000 and PVP-3000, respectively), and then PCE decreases to 3.66% with the further increase of the spin-coating speed to 5000 rpm (see Table 1). Thus, PCE of ITO/PEDOT:PSS/P3HT:PCBM/PVP/Al device shows the maximum (3.90%) at the optimum PVP spin-coating speed of 3000 rpm, which has a ca. 29% enhancement, compared to that of reference P3HT:PCBM device. Since the thickness of the PVP cathode buffer layer is determined by the spin-coating speed, these results indicate that the effect of the PVP cathode buffer

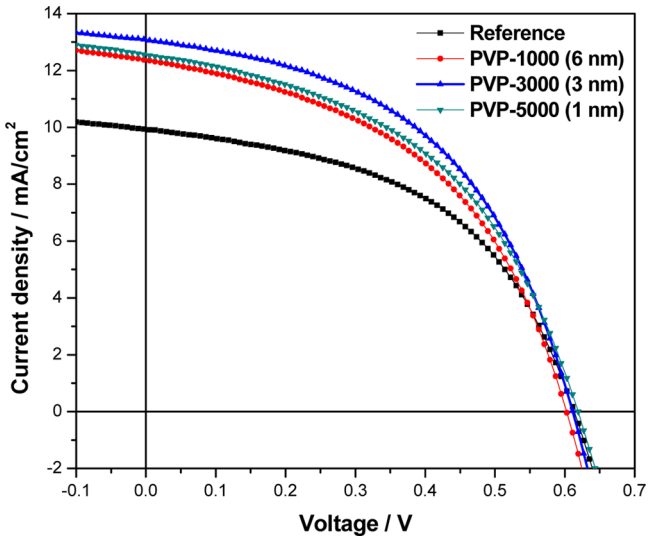

Figure 1. Current–voltage (J–V) curves of the ITO/PEDOT:PSS/P3HT:PCBM/PVP/Al BHJ-PSCs after thermal annealing with PVP buffer layers fabricated via spin coating at different speeds (1000, 3000, 5000 rpm, denoted as PVP-1000 (6 nm), PVP-3000 (3 nm), PVP-5000 (1 nm), respectively; the estimated thickness of PVP layer is included in the bracket) and without PVP buffer layer (reference). The measurements are carried out under AM 1.5 illumination at an irradiation intensity of 100 mW cm^{-2}.

dx.doi.org/10.1021/am302317v | ACS Appl. Mater. Interfaces 2013, 5, 26–34

Table 1. Photovoltaic Parameters of ITO/PEDOT:PSS/P3HT:PCBM/PVP/Al BHJ-PSCs with the PVP Cathode Buffer Layer Spin-Coated at Different Speeds (1000, 3000, 5000 rpm)[a]

No.	spin-coating speed (rpm)	V_{oc} (V)	J_{sc} (mA/cm^2)	FF (%)	PCE (%)	ΔPCE/PCE (%)[a]	R_s (Ω cm^2)	R_{sh} (Ω cm^2)
reference		0.61 ± 0.02	9.92 ± 0.3	50 ± 2	3.03 ± 0.12		14.3	316.5
PVP-1000	1000	0.60 ± 0.01	12.33 ± 0.3	47 ± 1	3.50 ± 0.03	16	12.1	232.8
PVP-3000	3000	0.61 ± 0.01	13.04 ± 0.3	49 ± 1	3.90 ± 0.03	29	11.6	275.4
PVP-5000	5000	0.62 ± 0.01	12.54 ± 0.3	47 ± 2	3.66 ± 0.06	21	13.3	245.3

[a]For each annealing condition, 6−10 devices were measured in order to obtain an average value. [a]ΔPCE/PCE is the enhancement ratio of PCE relative to the reference P3HT:PCBM BHJ-PSCs.

layer on the enhancement of the device performance is sensitively dependent on its thickness.

Each parameter used to determine PCE, including V_{oc}, J_{sc}, and FF, as well as the series resistance (R_s) and the shunt resistance (R_{sh}), is compared in detail in Table 1 to unveil the factor accounting for the enhancement of the PCE with the incorporation of PVP cathode buffer layer, and the dependence of the enhancements of each parameter on the PVP spin-coating speed is depicted in Figure 2. Clearly, V_{oc} of the PVP-

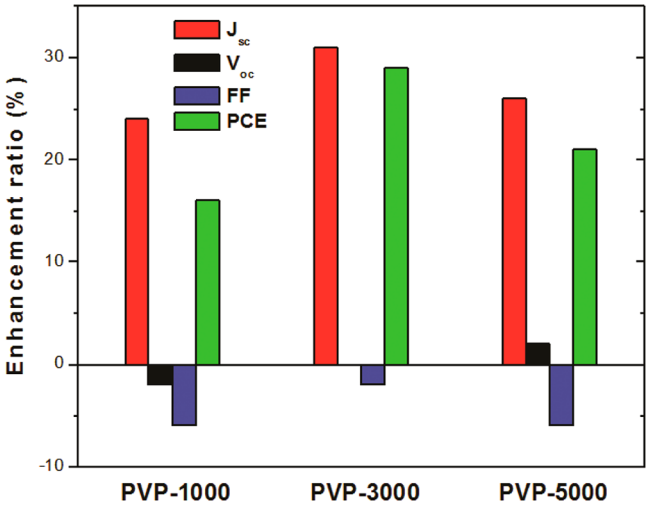

Figure 2. Enhancement ratio of the photovoltaic parameters of ITO/PEDOT:PSS/P3HT:PCBM/PVP/Al BHJ-PSC devices with PVP buffer layer fabricated via spin coating at different speeds.

incorporated devices remains almost constant (0.60−0.62 V), compared to that of the reference P3HT:PCBM device. This is essentially different to the cases of the reported cathode buffer layers based on PEO, PEG, PFN, and PDMS-*b*-PMMA, for which the dramatic increase of V_{oc} was attributed to the enhanced PCE of the corresponding devices.[27−30] On the other hand, J_{sc} of the PVP-incorporated devices increases dramatically by 31% from 9.92 mA/cm^2 to 13.04 mA/cm^2 for the PVP-3000 device, whereas FF decreases slightly from 50% to 47% (PVP-1000), 49% (PVP-3000), and 47% (PVP-5000). Interestingly, the series (R_s) and shunt resistance (R_{sh}) both decrease for the PVP-incorporated devices, compared to the reference P3HT:PCBM device (see Table 1). Again, this phenomenon is seldom observed in the reported studies of the cathode buffer layers based on PEO, PEG, PFN, and PDMS-*b*-PMMA, for which either both J_{sc} and FF increase simultaneously or only FF increases along with the increase of V_{oc}.[27−30]

Surface Morphologies of the PVP/P3HT:PCBM Bilayer Formed via Spin Coating. The surface morphologies of the P3HT:PCBM active layers with and without PVP buffer layer were first studied by SEM (see Figure S1 in the Supporting Information). The surface of the film of the P3HT:PCBM active layer within the reference device is quite smooth, according to the SEM image (see Figure S1a in the Supporting Information). Upon the incorporation of a PVP buffer layer fabricated under the optimum PVP spin-coating speed of 3000 rpm (PVP-3000), clearly there is an additional layer composed of aggregation domains on the P3HT:PCBM active layer (see Figure S1b in the Supporting Information). This result indicates the formation of PVP buffer layer on the surface of P3HT:PCBM layer due to the aggregation of PVP molecules. The formation of such aggregation domains is understandable, because PVP as a water-soluble nonconjugated polymer is more hydrophilic than both P3HT and PCBM,[34] and their difference on the hydrophilicity is confirmed by the water contact angle measurements, revealing that the water contact angle of the P3HT:PCBM film with PVP buffer layer (99°) is 10° smaller than that of the reference film without a PVP layer (see Figure S3 in the Supporting Information). This result indicates that the hydrophilic PVP buffer layer is indeed on the surface of P3HT:PCBM layer, enabling the P3HT:PCBM/PVP bilayer more hydrophilic with decreased water contact angle. The SEM measurement results combined with the water contact angle measurements confirm that spin-coating PVP onto the P3HT:PCBM active layer leads to the formation of the PVP buffer layer.

AFM in contact mode was then used to further investigate the surface morphologies of the P3HT:PCBM active layers with and without PVP buffer layer, indicating clearly P3HT-rich and PCBM-rich domains due to their microphase separation behavior while no discernible difference between the images with and without PVP buffer layer is found. This is presumably because both films are quite smooth and the difference on the image contrast of different components is too small under our instrumental conditions. The measured root-mean-square (RMS) roughness is 0.6−0.7 nm, which is comparable to those reported for the P3HT:PCBM BHJ-PSCs (see Figure S2 in the Supporting Information).[35] With such a small RMS roughness of the active layer, which is expected to be smaller than the thickness of the PVP cathode buffer layer, it is possible to estimate the thicknesses of the PVP cathode buffer layers on the top of the P3HT:PCBM active layer directly by AFM, which is obtained by subtracting the sum thickness of the PVP/P3HT:PCBM/PEDOT:PSS layer with that of the P3HT:PCBM/PEDOT:PSS layer (see Figure S4 in the Supporting Information). Accordingly, the thicknesses of the PVP cathode buffer layers are estimated to be 6, 3, and 1 nm for the PVP-1000, PVP-3000, and PVP-5000 devices, respectively. Based on the results on the effect of PVP layer thickness on the enhancement of the device performance as discussed above, it is clear that a PVP cathode buffer layer in the thickness range of 1−6 nm is beneficial for the performance of the P3HT:PCBM

device, with a 3-nm thickness being optimum. A thicker PVP cathode buffer layer would prohibit the charge transport from active layer to the cathode electrode, because PVP is an insulating nonconjugated polymer, whereas a thinner PVP interlayer would be inferior for its impact on the charge collection, as discussed below. This conclusion is consolidated by our comparative study of the influence of the solvent dissolving PVP on its effect. When isopropyl alcohol was used for spin-coating PVP layer under the same spin-coating speed (3000, 5000 rpm), both devices with a PVP layer incorporated indicate obvious decreases of the PCE, even compared to the reference device (see Figure S5 and Table S1 in the Supporting Information), suggesting that the PVP layer thus formed is too thick, compared to that spin-coated from the methanol solvent, because the volatility of isopropyl alcohol is much lower than that of methanol.

Effect of the PVP Cathode Buffer Layer on the Enhancement of the Device Performance. Generally, the $J-V$ curve in the darkness provides valuable information of the inherent electrical characteristics of the BHJ-PSC devices, including the series resistance (R_s), the shunt resistance (R_{sh}), the leakage current, and the saturation current density.[1−9,36−38] Figure 3 presents the $J-V$ curves of ITO/PEDOT:PSS/P3HT:PCBM/PVP/Al devices in the darkness, in comparison with that of the reference device. Evidently, the dark currents of PVP-incorporated devices of PVP-3000 and PVP-5000 are dramatically higher than those of the reference device in both reverse and forward regions, and these results are in good accordance with the decreases of both R_s and R_{sh} for the PVP-incorporated devices (see Table 1). Even for the PVP-1000 device with a 6-nm-thick PVP cathode buffer layer, the dark currents are also higher than those of the reference device, with the bias voltage exceeding a threshold (−0.48 and 0.32 V for reverse and forward region, respectively), and both the R_s and R_{sh} values of the PVP-1000 device are smaller than those of the reference device (see Table 1). Note that the decrease in R_s upon incorporation of the PVP interlayer confirms that PVP fulfills the prerequisite of an ideal material as a cathode buffer layer. On the other hand, the decrease in R_{sh} is presumably due to the increase of the surface roughness of the Al electrode, as discussed below, resulting in the increase of leakage current, as illustrated in Figure 3.

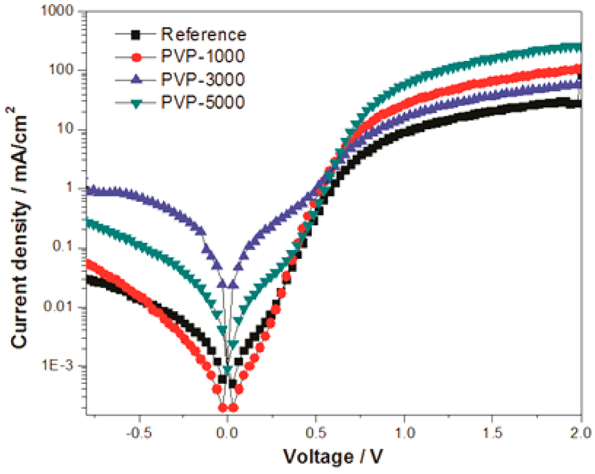

Figure 3. $J-V$ curve of the ITO/PEDOT:PSS/P3HT:PCBM/PVP/Al BHJ-PSCs in the dark with and without PVP buffer layers fabricated via spin coating at different speeds.

It is well-known that charge collection efficiency of the BHJ-PSC device is primarily determined not only by the electrodes but also by the interfaces. Considering the electron extraction that occurs between the interface of the active layer and the cathode electrode, ideally, the maximum efficiency of electron extraction can be achieved when the work function of the cathode is aligned with the LUMO level of the acceptor, to form ohmic contact. However, for the standard reference ITO/PEDOT:PSS/P3HT:PCBM/Al devices, there is a significant energy level offset (0.3 eV) between the work function of Al (4.3 eV) and the LUMO level of the PCBM acceptor (4.0 eV) (see Scheme 2), resulting in unfavorable electron extraction.[1−15] Moreover, numerous previous reports reveal that a strong interaction between Al and the thiophene rings of P3HT may happen and consequently disrupt the conjugation of the P3HT main chain. As a result, the highest PCE of P3HT:PCBM BHJ-PSCs as the most widely studied structure is limited to 5.2%.[39] In order to optimize the interfaces between the PCBM acceptor and the Al cathode, cathode buffer layers (such as LiF, PEO, PFN, and PEG) have been incorporated to facilitate electron collection and extraction by means of inducing interfacial charge redistribution, geometry modifications, and/or chemical reactions.[11−17,27−29,40]

Scheme 2. Schematic Energy Level Diagram of ITO/PEDOT:PSS/P3HT:PCBM/Al BHJ-PSC Devices with the Incorporation of a PVP Buffer Layer

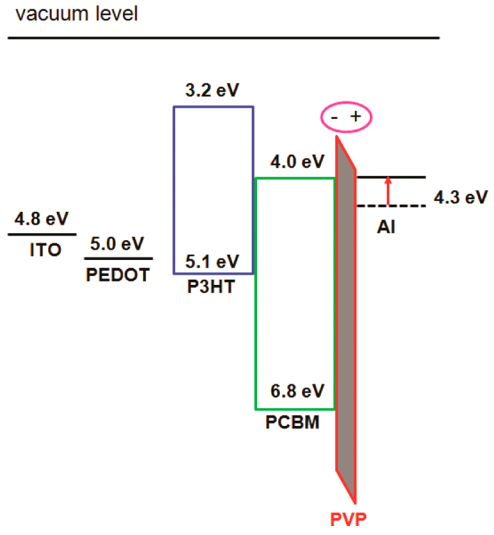

PVP is an insulating nonconjugated polymer with a strong dipole moment (4.07 D),[41] which results from the side chain of pyrrolidone. Based on the above analysis that the incorporation of PVP cathode buffer layer facilitates the charge collection leading to the enhancement of the PCE of the P3HT:PCBM BHJ-PSCs, it is reasonable to assume, intuitively, that, similar to the cases of PEO and PFN,[27,28] the insertion of a PVP interlayer would readily lead to the formation of a dipole layer, which consequently reduces the work function of Al. This assumption was experimentally confirmed by the SKPM measurements (see Figure S6 in the Supporting Information). Clearly, the surface potential of the P3HT:PCBM/PVP layer within the PVP-3000 device is ca. 250 mV more positive than that of the P3HT:PCBM active layer within the reference

dx.doi.org/10.1021/am302317v | ACS Appl. Mater. Interfaces 2013, 5, 26−34

device without PVP incorporation. This result is reasonably consistent with that observed in the PFN interlayer used in PTB7/PC71BM device reported in ref 28, thus confirming the formation of the dipole layer of PVP in our PVP-incorporated devices, for which the positive charge end points toward the Al electrode and the negative charge end points toward the P3HT:PCBM photoactive layer (see Scheme 2).[28] As a result, the energy level offset between the work function of Al and the LUMO level of the PCBM acceptor is decreased, facilitating electron extraction by the Al cathode. To this effect of dipole layer formation, we believe that the strong dipole moment of PVP is essential.

Given that there are lone-pair electrons on the oxygen atoms of the pyrrolidone side chain of PVP, the interactions between the lone-pair electrons on the oxygen atoms with Al atoms as proposed for the PEG-incorporated devices should contribute to the effect of PVP cathode buffer layer on the efficiency enhancement of the devices as well.[29,40] In fact, PVP has been extensively used as a polymeric capping agent whose oxygen atoms bind strongly with metals such as Ag and Pd.[42] Hence, we expect that PVP interacts strongly with Al atoms via such a capping effect, i.e., the coordination of oxygen atoms with Al atoms. As a result, the strong interaction between the Al and the thiophene rings of P3HT, which may disrupt the conjugation of P3HT, can be prohibited, because of the protection of the PVP interlayer. Besides, the contact resistance between active layer and Al cathode is reduced after the chemical reactions of PVP with Al atoms, facilitating the electron collection by the Al cathode.

Among the determinative parameters of PCE of BHJ-PSCs, including V_{oc}, J_{sc}, and FF, V_{oc} is primarily correlated to the difference between the HOMO level of the donor and the LUMO level of the acceptor within the active layer; J_{sc} is dependent not only on the multiplication of the photo-induced charge carrier density and the charge carrier mobility within the active material but also on the interface properties between the active layers and the electrodes; FF is determined by charge carriers reaching the electrodes, when the built-in field is reduced toward the open-circuit voltage.[1−15] With the above interpretations on the effect of the PVP cathode buffer layer, including not only the formation of a dipole layer between the P3HT:PCBM active layer and Al electrodes but also the chemical reactions of PVP with Al atoms, the influence of PVP on each parameter can be analyzed further. As mentioned above, in the previous reports on the cathode buffer layers based on PEO, PEG, PFN, and PDMS-*b*-PMMA, typically V_{oc} increases and either both J_{sc} and FF increase simultaneously or only FF increases along with the increase of V_{oc}.[27−30] For our present case of a PVP cathode buffer layer, only J_{sc} increases, whereas V_{oc} remains almost unchanged and FF even decreases instead (see Figure 2). Thus, other effects should be taken into consideration.

To probe the influence of PVP cathode buffer layer on the top Al electrode in addition to the interface between PVP and P3HT:PCBM (PVP/P3HT:PCBM), we compared the morphology of the top Al film with and without the PVP cathode buffer layer by AFM. Surprisingly, the top Al film deposited onto the PVP/P3HT:PCBM bilayer of PVP-3000 device shows a dramatic increase in roughness (5.41 nm), compared to that for the reference ITO/PEDOT:PSS/P3HT:PCBM/Al device (3.43 nm) (see Figure S7 in the Supporting Information). This presumably resulted from the facile chemical reactions of PVP with Al atoms, as discussed above. With the increase of the roughness of the top Al film, the interface between the P3HT:PCBM active layer and the Al electrode is further interrupted by the PVP buffer layer; as a result, the charge accumulation and, consequently, recombination loss of charge carriers may easily take place at the interface of P3HT:PCBM and Al (P3HT:PCBM/Al), leading to a decrease in the number of charge carriers reaching the Al electrode (i.e., a decrease in FF). Nevertheless, attributed to more dominant effects that the incorporation of PVP cathode buffer layer leads not only to the formation of a dipole layer between P3HT:PCBM active layer and Al electrodes but also to the chemical reactions of PVP with Al atoms, the overall effect of PVP cathode buffer layer is the increase of the charge carriers collected by the Al electrode; therefore, an overwhelming increase in J_{sc} is observed. Finally, V_{oc} remains almost unchanged, presumably because of the tradeoff between the increase in V_{oc}, which is due to the increased built-in potential upon the formation of an interfacial dipole layer, and the decrease in V_{oc}, which resulted from the increased leakage current, as discussed above.[28]

Formation of PVP Cathode Buffer Layer by Self-Assembly. In order to address whether or not the effect of the PVP cathode buffer layer on the enhancement of the PCE of the P3HT:PCBM BHJ-PSCs device is dependent on the fabrication method, we next studied the alternative method of incorporating PVP by doping it directly into the P3HT:PCBM active layer (see method (II) in Scheme 1). PVP was dissolved in chlorobenzene and doped into a P3HT:PCBM solution in chlorobenzene with variable weight ratios (1, 3, 5 wt %), which was used as the active layer for the device fabrication (denoted as PVP-1%, PVP-3%, and PVP-5%, respectively). Following the so-called "slow drying" or "slow growth" method[43] used in the literature of incorporating PEG[29] or the fullerene end-capped PEG[31,32] as the cathode buffer layer, we used the same technique to fabricate the PVP-doped P3HT:PCBM active layer in order to facilitate the migration of PVP molecules to the interface, which is believed to be beneficial for an increased hole mobility and balanced charge transport.[43]

The surface morphologies of the PVP-doped P3HT:PCBM active layer (PVP-3%) is measured by both SEM and AFM and compared with that of the reference device (see Figure S8 in the Supporting Information). As clearly seen from the comparison of the SEM images of P3HT:PCBM films with and without 3% PVP doping (see panel I in Figure S8 in the Supporting Information), the PVP-doped P3HT:PCBM film exhibits randomly distributed spherical particles, which is absent in the image of the reference film. Interestingly, the formation of spherical particles found in the PVP-doped P3HT:PCBM film is quite similar to the reported PEG or the fullerene end-capped PEG as the cathode buffer layer, which were both doped into the P3HT:PCBM active layer first and subsequently migrated onto the surface of the P3HT:PCBM layer.[29,31] This result suggests that, analogous to the case of PEG and the fullerene end-capped PEG, PVP molecules doped in the P3HT:PCBM active layer may undergo self-assembly and migrate to the surface of the P3HT:PCBM active layer, causing the formation of the PVP cathode buffer layer, which has a similar effect to the PVP interlayer spin-coated onto the active layer, leading to the efficiency enhancement of BHJ-PSC devices. Such an assumption of formation of the PVP cathode buffer layer via self-assembly after doping in active layers was confirmed by AFM and water contact angle measurements. According to the comparison of the AFM images of P3HT:PCBM films with and without PVP doping (see panel

II in Figure S8 in the Supporting Information), the overall morphology of PVP-doped P3HT:PCBM film is obviously different than the reference one, and a RMS roughness of ~0.68 nm measured for the PVP-doped P3HT:PCBM film is much smaller than that of the reference (undoped) one (1.38 nm), revealing that the surface morphology of P3HT:PCBM film changes dramatically upon the doping of PVP. Since PVP is doped in the P3HT:PCBM layer at a very low doping ratio (3%), a dramatic change of the morphology of P3HT:PCBM layer would be unlikely if PVP molecules reside within the P3HT:PCBM layer; therefore, the migration of PVP molecules via self-assembly to the surface of the P3HT:PCBM layer should be responsible for the observed dramatic change of the morphology of P3HT:PCBM layer. Moreover, the measured water contact angle of the PVP-doped P3HT:PCBM film is 100°, which is 9° smaller than that of the reference (undoped) film (see Figure S3 in the Supporting Information). This result indicates that the hydrophilicity of P3HT:PCBM film is dramatically affected by PVP doping and this is due to the migration of PVP molecules via self-assembly to the surface of the P3HT:PCBM layer. Interestingly, the measured water contact angle of the PVP-doped P3HT:PCBM film is quite comparable to that of the P3HT:PCBM/PVP bilayer in which PVP buffer layer was spin-coated directly on the P3HT:PCBM layer, suggesting that a similar P3HT:PCBM/PVP bilayer structure exists for the PVP-doped P3HT:PCBM film.

The $J-V$ curves of the annealed ITO/PEDOT:PSS/PVP:P3HT:PCBM/Al BHJ-PSC devices are compared in Figure 4 and the measured parameters (J_{sc}, V_{oc}, FF, PCE) are

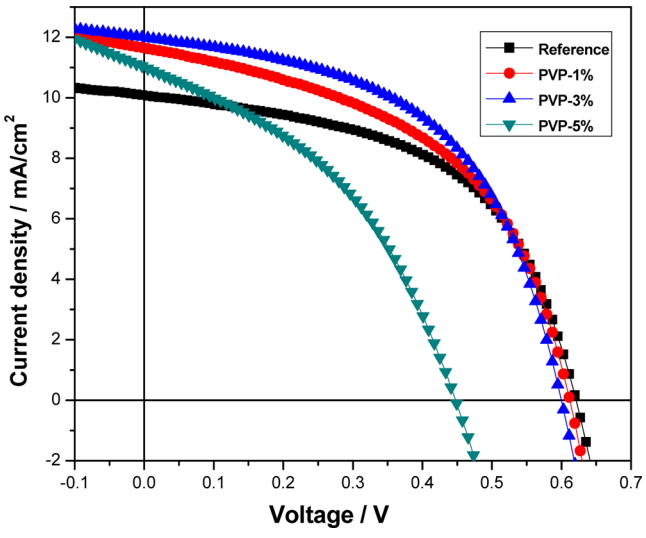

Figure 4. $J-V$ curves of the ITO/PEDOT:PSS/P3HT:PCBM:PVP/Al BHJ-PSCs without PVP doping (black) and with PVP doped in P3HT:PCBM solution in chlorobenzene with different ratios of 1, 3, and 5 wt % (denoted as PVP-1%, PVP-3%, and PVP-5%, respectively). The measurements are carried out under AM 1.5 illumination at an irradiation intensity of 100 mW cm^{-2}.

summarized in Table 2. Compared to the reference (undoped) ITO/PEDOT:PSS/P3HT:PCBM/Al device, which has a PCE of 3.36%, the PVP-doped devices PVP-1% and PVP-3% show an obviously enhanced PCE of 3.53% and 3.78%, respectively. Interestingly, it is found that the enhancement of PCE of PVP-1% (3%) is mainly attributed to the increase of J_{sc}, whereas V_{oc} remains almost unchanged and FF slightly decreases, and this phenomenon is exactly same as that for the PVP interlayer spin-coated onto the active layer. These results further confirm our above conclusion that PVP molecules doped in a P3HT:PCBM active layer migrate to the top of the P3HT:PCBM active layer via self-assembly. Thus, a similar effect of PVP self-assembly layer on the efficiency enhancement of BHJ-PSC devices is applicable. Note that, however, a higher doping ratio of PVP to 5% leads to a dramatic decrease in the PCE (2.03%), suggesting that overloading of PVP in the active layer should be avoided. This is understandable, because PVP is insulating and its overloading would increase series resistance (R_s) of the device from 11.1 Ω cm^2 to 15.3 Ω cm^2 and, consequently, lower the FF from 54% to 41%. In fact, for the PEG cathode buffer layer, it was reported that a doping ratio of 5 wt % led to an enhancement of the PCE of P3HT:PCBM devices by ca. 71%, while 10 wt % PEG doping decreased the PCE, compared to the reference device.[29] These results indicate that the effect of PVP on the device performance is somewhat different to that of PEG, and this is naturally originated from their difference on the molecular structure and dipole moment, as discussed above.

With a relatively low PVP doping ratio (1−3 wt %), the thickness of the PVP cathode buffer layer formed by self-assembly is expected to be limited, while its effect on the enhancement of the device performance is clearly detected. Indeed, the thickness of the PVP layer formed by self-assembly for PVP-3% is determined to be ca. 6 nm, which is much larger than that for PVP-3000 (3 nm). By lowering the doping ratio of PVP within P3HT:PCBM layer, it is, in principle, possible to obtain a comparable thickness of PVP self-assembly layer to that for PVP-3000 (3 nm); however, the measured PCE of the PVP-1% device is even lower than that for the PVP-3% device. Although a PVP cathode buffer layer forms in both cases (self-assembly and spin coating), it is inappropriate to compare their device performances directly, because the method used to fabricate the P3HT:PCBM active layer is different for the case of incorporating a PVP interlayer via self-assembly or spin coating.[43] Indeed, we also studied the fabrication of PVP-doped P3HT:PCBM BHJ-PSC devices, using the conventional "fast growth" method, and the ITO/PEDOT:PSS/P3HT:PCBM:PVP/Al BHJ-PSC devices fabricated under different PVP doping ratios of 1, 3, and 5 wt % all show decreased PCE values (2.64%, 1.59%, and 0.94%, respectively), compared to the reference device (3.08%). Nevertheless, according to our results, the dependence of the enhancement of the device performance on the thickness of the PVP cathode buffer layer formed by self-assembly or spin coating is obviously different, and this can be understood by considering the different aggregation microstructures of PVP interlayer formed by self-assembly or spin coating, as revealed by the SEM study discussed above.

CONCLUSIONS

In summary, for the first time, we applied a nonconjugated polymer poly(vinylpyrrolidone) (PVP) as a new cathode buffer layer in P3HT:PCBM BHJ-PSCs, resulting in the significant efficiency enhancement. PVP was incorporated between the P3HT:PCBM active layer and Al electrode by means of either spin coating or self-assembly. For the case of incorporation of PVP by spin coating, the PCE of the ITO/PEDOT:PSS/P3HT:PCBM/PVP/Al BHJ-PSC device (3.90%) is enhanced by 29% under the optimum PVP spin-coating speed of 3000 rpm, which is primarily due to the increase in J_{sc} (31% enhancement), suggesting the increase of the charge collection upon the incorporation of a PVP cathode buffer layer. The

dx.doi.org/10.1021/am302317v | ACS Appl. Mater. Interfaces 2013, 5, 26−34

Table 2. Photovoltaic Parameters of ITO/PEDOT:PSS/P3HT:PCBM:PVP/Al BHJ-PSCs with PVP Doped in the P3HT:PCBM Active Layer at Different Ratios (1, 3, and 5 wt %)[a]

No.	doping ratio of PVP (%)[b]	V_{oc} (V)	J_{sc} (mA/cm^2)	FF (%)	PCE (%)	ΔPCE/PCE (%)[c]	R_s (Ω cm^2)	R_{sh} (Ω cm^2)
reference		0.62 ± 0.04	10.07 ± 0.3	54 ± 2	3.36 ± 0.24		11.1	346.2
PVP-1%	1	0.61 ± 0.01	11.63 ± 0. 3	50 ± 1	3.53 ± 0.03	5	10.2	213.5
PVP-3%	3	0.60 ± 0.02	11.98 ± 0.2	53 ± 1	3.78 ± 0.04	13	9.8	309.4
PVP-5%	5	0.45 ± 0.03	11.01 ± 0.3	41 ± 2	2.03 ± 0.18	−40	15.3	104.7

[a]The BHJ-PSC devices were fabricated by the "slow drying" technique. For each annealing condition, 6−10 devices were measured in order to obtain an average value. [b]PVP:P3HT:PCBM = X mg:1 mg:0.8 mg, where X = 0, 0.018, 0.054, and 0.090. The doping ratio of PVP = $X/(1 + 0.8)$. [c]ΔPCE/PCE is the enhancement ratio of PCE relative to the reference P3HT:PCBM BHJ-PSCs.

influence of a PVP cathode buffer layer on the efficiency enhancement is interpreted by the conjunct effects of the formation of a dipole layer between P3HT:PCBM active layer and Al electrodes, the chemical reactions of PVP molecules with Al atoms, and the increase of the roughness of the top Al film. Noteworthy, the latter effect leads to a slight decrease in FF, which has been hardly observed in reported cathode buffer layers, based on other nonconjugated insulating polymers. The thickness of the PVP cathode buffer layer plays an important role in its effect on the charge collection, with a thickness of 3 nm being optimum. Incorporation of a PVP layer by doping PVP directly into the P3HT:PCBM active layer was also studied, to address whether its effect is dependent on the fabrication method. An enhancement of PCE by 13% was achieved under the optimum PVP doping ratio of 3%, and this is interpreted by the migration of PVP molecules to the surface of the active layer via self-assembly, resulting in the formation of the PVP cathode buffer layer as well. While the formation of the PVP cathode buffer layer is fulfilled by both fabrication methods (spin coating and self-assembly), the dependence of the enhancement of the device performance on the thickness of the PVP cathode buffer layer formed by self-assembly or spin coating is different, because of the different aggregation microstructures of the PVP interlayer. With the effectiveness of PVP as a cathode buffer layer, this study provides not only a simple and facile strategy for efficiency enhancement of polymer solar cells but also new insights into the essentiality of the interfacial layers.

■ ASSOCIATED CONTENT

Supporting Information

Surface morphology of P3HT:PCBM films with and without PVP incorporation; determination of the thickness of the PVP cathode buffer layers by AFM; $J-V$ curves and photovoltaic parameters of P3HT:PCBM BHJ-PSCs with PVP cathode buffer layer incorporated via spin coating from different solvents (methanol versus isopropyl alcohol); surface potential images measured by SKPM; surface morphology of the top Al film by AFM, etc. This material is available free of charge via the Internet at http://pubs.acs.org.

■ AUTHOR INFORMATION

Corresponding Author

*E-mail: sfyang@ustc.edu.cn.

Notes

The authors declare no competing financial interest.

■ ACKNOWLEDGMENTS

Technical assistances of Mr. Jianliu Huang, Mr. Xuefei Feng, Dr. Ying Xiong and valuable discussions with Prof. Junfa Zhu, and Prof. Yangchao Tian (NSRL) are cordially acknowledged. We thank the financial support from the National Natural Science Foundation of China (Nos. 90921013 and 21132007), "100 Talents Programme of CAS" from Chinese Academy of Sciences, USTC-NSRL Association Funding (No. KY2060140003), the Fundamental Research Funds for the Central Universities (No. WK2060140005), Key Laboratory of Novel Thin Film Solar Cells (No. KF201103), Chinese Academy of Sciences, "Specialized Research Fund for the Doctoral Program of Higher Education" (No. 20113402110020) and National Basic Research Program of China (Nos. 2010CB923300 and 2011CB921400).

■ REFERENCES

(1) Thompson, B. C.; Fréchet, J. M. J. *Angew. Chem., Int. Ed.* **2008**, *47*, 58−77.
(2) Dennler, G.; Scharber, M. C.; Brabec, C. J. *Adv. Mater.* **2009**, *21*, 1323−1338.
(3) Krebs, F. C.; Fyenbo, J.; Jørgensen, M. *J. Mater. Chem.* **2010**, *20*, 8994−9001.
(4) Deibel, C.; Dyakonov, V. *Rep. Prog. Phys.* **2010**, *73*, 096401−1-39.
(5) Cai, W. Z.; Gong, X.; Cao, Y. *Solar Energy Mater. Solar Cells* **2010**, *94*, 114−127.
(6) Zheng, Y.; Xue, J. G. *Polym. Rev.* **2010**, *50*, 420−453.
(7) Siddiki, M. K.; Li, J.; Galipeau, D.; Qiao, Q. Q. *Energy Environ. Sci.* **2010**, *3*, 867−883.
(8) He, Y. J.; Li, Y. F. *Phys. Chem. Chem. Phys.* **2011**, *13*, 1970−1983.
(9) Li, G.; Zhu, R.; Yang, Y. *Nat. Photon.* **2012**, *6*, 153−161.
(10) Dang, M. T.; Hirsch, L.; Wantz, G. *Adv. Mater.* **2011**, *23*, 3597−3602.
(11) Po, R.; Carbonera, C.; Bernardi, A.; Camaioni, N. *Energy Environ. Sci.* **2011**, *4*, 285−310.
(12) Steim, R.; Kogler, F. R.; Brabec, C. J. *J. Mater. Chem.* **2010**, *20*, 2499−2512.
(13) Chen, L. M.; Xu, Z.; Hong, Z. R.; Yang, Y. *J. Mater. Chem.* **2010**, *20*, 2575−2598.
(14) Ma, H.; Yip, H. L.; Huang, F.; Jen, A. K. *Adv. Funct. Mater.* **2010**, *20*, 1371−1388.
(15) Yip, H. L.; Jen, A. K. *Energy Environ. Sci.* **2012**, *5*, 5994−6011.
(16) Brabec, C. J.; Shaheen, S. E.; Winder, C.; Sariciftci, N. S.; Denk, P. *Appl. Phys. Lett.* **2002**, *80*, 1288−1290.
(17) Chen, X.; Zhao, C.; Rothberg, L.; Ng, M.-K. *Appl. Phys. Lett.* **2008**, *93*, 123302-1−123302-3.
(18) Kim, J. Y.; Kim, S. H.; Lee, H.-H.; Lee, K.; Ma, W. L.; Gong, X.; Heeger, A. J. *Adv. Mater.* **2006**, *18*, 572−576.
(19) Kim, J. Y.; Lee, K.; Coates, N. E.; Moses, D.; Nguyen, T.; Dante, M.; Heeger, A. J. *Science* **2007**, *317*, 222−225.
(20) Oh, S. H.; Na, S. I.; Jo, J.; Lim, B.; Vak, D.; Kim, D. Y. *Adv. Funct. Mater.* **2010**, *20*, 1977−1983.
(21) Nickel, F.; Puetz, A.; Reinhard, M.; Do, H.; Kayser, C.; Colsmann, A.; Lemmer, U. *Org. Electron.* **2010**, *11*, 535−538.
(22) Stevens, D. M.; Qin, Y.; Hillmyer, M. A. *J. Phys. Chem. C.* **2009**, *113*, 11408−11415.
(23) Tremolet de Villers, B.; Tassone, C. J.; Tolbert, S. H.; Schwartz, B. J. *J. Phys. Chem. C.* **2009**, *113*, 18978−18982.

(24) Chen, X.; Yang, J.; Lu, J.; Manga, K. K.; Loh, K. P.; Zhu, F. *Appl. Phys. Lett.* **2009**, *95*, 133305-1−133305-3.
(25) Kim, J.-H.; Huh, S.-Y.; Kim, T.-I.; Lee, H. H. *Appl. Phys. Lett.* **2008**, *93*, 143305-1−143305-3.
(26) Wei, Q.; Nishizawa, T.; Tajima, K.; Hashimoto, K. *Adv. Mater.* **2008**, *20*, 2211−2216.
(27) Zhang, F. L.; Ceder, M.; Inganäs, O. *Adv. Mater.* **2007**, *19*, 1835−1838.
(28) He, Z. C.; Zhong, C. M.; Huang, X.; Wong, W.-Y.; Wu, H. B.; Chen, L. W.; Su, S. J.; Cao, Y. *Adv. Mater.* **2011**, *23*, 4636−4643.
(29) Chen, F.-C.; Chien, S.-C. *J. Mater. Chem.* **2009**, *19*, 6865−6869.
(30) Yamakawa, S.; Tajima., K.; Hashimoto, K. *Org. Electron.* **2009**, *10*, 511−514.
(31) Jung, J. W.; Jo, J. W.; Jo, W. H. *Adv. Mater.* **2011**, *23*, 1782−1787.
(32) Tai, Q. D.; Li, J. H.; Liu, Z. K.; Sun, Z. H.; Zhao, X. Z.; Yan, F. *J. Mater. Chem.* **2011**, *21*, 6848−6853.
(33) Zhang, W. F.; Xu, Y.; Wang, H. T.; Xu, C. H.; Yang, S. F. *Solar Energy Mater. Solar Cells* **2011**, *95*, 2880−2885.
(34) Haaf, F.; Sanner, A.; Straub, F. *Polym. J.* **1985**, *17*, 143−152.
(35) Lee, D.; Park, J.; Noh, S.; Kim, J.; Lee, S.; Lee, C. *Thin Solid Films* **2009**, *518*, 541−544.
(36) Waldauf, C.; Scharber, M. C.; Schilinsky, P.; Hauch, J. A.; Brabec, C. J. *J. Appl. Phys.* **2006**, *99*, 104503-1−104503-6.
(37) Lee, M.-K.; Wang, J.-C.; Horng, S.-F.; Meng, H.-F. *Solar Energy Mater. Solar Cells* **2010**, *94*, 114−127.
(38) Guan, X.; Zhang, K.; Huang, F.; Bazan, G. C.; Cao, Y. *Adv. Funct. Mater.* **2012**, *22*, 2846−2854.
(39) Irwin, M. D.; Buchholz, D. B.; Hains, A. W.; Chang, R. P. H.; Marks, T. J. *Proc. Natl. Acad. Sci. U.S.A.* **2008**, *105*, 2783−2787.
(40) Deng, X.; Lau, W.; Wong, K. *Appl. Phys. Lett.* **2004**, *84*, 3522−3524.
(41) Oh, S. H.; Ryoo, R.; John, M. S. *Macromolecules* **1990**, *23*, 1671−1675.
(42) Xia, Y. N.; Xiong, Y. J.; Lim, B. K.; Skrabalak, S. E. *Angew. Chem., Int. Ed.* **2009**, *48*, 60−103.
(43) Li, G.; Shrotriya, V.; Huang, J. S.; Yao, Y.; Moriarty, T.; Emery, K.; Yang, Y. *Nat. Mater.* **2005**, *4*, 864−868.